Abstract: Monoclinic Y_2SiO_5 was found to be an attractive, simultaneously laser and $\chi^{(3)}$-nonlinear active optical crystal. Passively Q-switched LD-pumped nanosecond Nd^{3+}:Y_2SiO_5 self-Raman laser, operating by nonlinear-cascaded scheme is reported. We achieved also quasi-CW generation of Y_2SiO_5:Nd^{3+} at 1.3585 μm. Many-wavelength Raman-induced $\chi^{(3)}$-lasing in undoped Y_2SiO_5 under picosecond excitation has been observed, as well. All recorded Stokes and anti-Stokes components were identified and attributed to SRS-promoting vibration modes. Gives a short review of self-Raman lasers and laser potential of rare-earth C_{2h}^6-monoclinic orthosilicates doped with Ln^{3+} lasants.

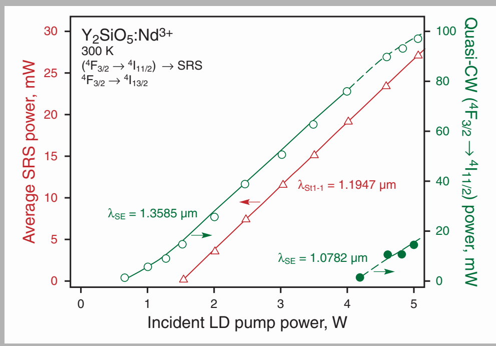

The dependences of the average output power versus incident pump power at $\lambda_p \approx 0.809$ μm wavelength of the nanosecond Nd^{3+}:Y_2SiO_5 self-Raman laser at $\lambda_{St1-1} = 1.1947$ μm (shown by triangles) and of the quasi-CW Nd^{3+}:Y_2SiO_5 laser at wavelengths of $\lambda_{SE} = 1.3585$ μm ($^4F_{3/2} \rightarrow {}^4I_{13/2}$) and $\lambda_{SE} = 1.0782$ μm ($^4F_{3/2} \rightarrow {}^4I_{11/2}$)

New passively Q-switched LD-pumped self-Raman laser with single-step cascade SE → SRS wavelength conversion on the base of monoclinic Nd^{3+}:Y_2SiO_5 crystal

A.A. Kaminskii, [1,*] *S.N. Bagayev,* [2] *K. Ueda,* [3,**] *J. Dong,* [4] *and H.J. Eichler* [5]

[1] Institute of Crystallography, Russian Academy of Sciences, Moscow 119333, Russia
[2] Institute of Laser Physics, Russian Academy of Sciences, Novosibirsk 630090, Russia
[3] Institute for Laser Science, University of Electro-Communications, 182-8585 Tokyo, Japan
[4] Department of Electronic Engineering, School of Information Science and Technology, Xiamen University, Xiamen 361005, China
[5] Institute of Optics and Atomic Physics, Technical University Berlin, Berlin 10623, Germany

Received: 17 November 2009, Accepted: 20 November 2009
Published online: 8 February 2010

Key words: self-Raman laser; Y_2SiO_5:Nd^{3+} laser crystals; cascaded nonlinear lasing; passive Q-switching; stimulated Raman scattering; stimulated emission; laser-diode pumping

PACS: 42.55.Xi, 42.55.Rz, 42.60.Lh, 42.55.Ye, 43.65.Dr, 42.60.Gd, 42.70.Hj

1. Introduction

Crystalline self-Raman lasers (SRL) are an attractive alternative to conventional inter-cavity Raman lasers with a separate SE-active (SE: stimulated emission) active Ln^{3+}-ion doped crystal and SRS-active (SRS: stimulate Raman scattering) frequency $\chi^{(3)}$-converter. Self-Raman lasers with laser-exhibit much lower reflection and scattering losses, as well as having a simpler and more robust cavity

* Corresponding author: e-mail: kaminalex@mail.ru, ** ueda@ils.uec.ac.jp

Crystal	Space group	SE			SRS		Ref. [a]
		Ln^{3+}	SE channel	λ_{SE}, μm	ω_{SRS}, cm^{-1}	λ_{St1}, μm	
α-$KY(WO_4)_2$	C_{2h}^6	Nd^{3+}	$^4F_{3/2} \rightarrow {}^4I_{11/2}$	1.0688	≈ 905	≈ 1.183	[1]
		Yb^{3+}	$^2F_{5/2} \rightarrow {}^2F_{7/2}$	≈ 1.029		≈ 1.136	[2]
		Tm^{3+}	$^3H_4 \rightarrow {}^3H_6$	≈ 1.95		≈ 2.365	[3]
α-$KGd(WO_4)_2$	C_{2h}^6	Pr^{3+}	$^1D_2 \rightarrow {}^3F_4$	1.0657	≈ 901	≈ 1.179	[4]
		Nd^{3+}	$^4F_{3/2} \rightarrow {}^4I_{11/2}$	1.0672	≈ 901	≈ 1.181	[1,5,6]
					≈ 768	≈ 1.162	[5,7]
			$^4F_{3/2} \rightarrow {}^4I_{13/2}$	≈ 1.351	≈ 901	≈ 1.538	[5,8,9]
		Yb^{3+}	$^2F_{5/2} \rightarrow {}^2F_{7/2}$	≈ 1.033	≈ 901	≈ 1.139	[10]
α-$KLu(WO_4)_2$	C_{2h}^6	Nd^{3+}	$^4F_{3/2} \rightarrow {}^4I_{11/2}$	1.0702	≈ 907	1.1852	[4]
		Yb^{3+}	$^2F_{5/2} \rightarrow {}^2F_{7/2}$	1.0306		1.1376	[11]
$KY(MoO_4)_2$	D_{2h}^{14}	Nd^{3+}	$^4F_{3/2} \rightarrow {}^4I_{11/2}$	1.0669	≈ 868	1.1852	[4]
					≈ 947	1.1868	[4]
$Ca(NbO_2)_3$	D_{2h}^{14}	Nd^{3+}	$^4F_{3/2} \rightarrow {}^4I_{11/2}$	1.0615	≈ 904	1.1741	[12]
$CaMoO_4$	C_{4h}^6	Nd^{3+}	$^4F_{3/2} \rightarrow {}^4I_{11/2}$	1.0576	≈ 879	≈ 1.166	[13]
$SrMoO_4$	C_{4h}^6	Nd^{3+}	$^4F_{3/2} \rightarrow {}^4I_{11/2}$	1.0576	≈ 886	≈ 1.167	[13]
$SrWO_4$	C_{4h}^6	Nd^{3+}	$^4F_{3/2} \rightarrow {}^4I_{11/2}$	≈ 1.057	≈ 922	≈ 1.171	[13,14]
Y_2SiO_5	C_{2h}^6	Nd^{3+}	$^4F_{3/2} \rightarrow {}^4I_{11/2}$	1.0782	≈ 904	1.1947	**this work**
YVO_4	C_{4h}^{19}	Nd^{3+}	$^4F_{3/2} \rightarrow {}^4I_{11/2}$	1.0641	≈ 890 [b]	1.1754	[15]
			$^4F_{3/2} \rightarrow {}^4I_{13/2}$	≈ 1.342		≈ 1.525	[16]
		Yb^{3+}	$^2F_{5/2} \rightarrow {}^2F_{7/2}$	≈ 1.014	≈ 892	≈ 1.115	[17]
β-$LaBGeO_2$	C_3^2	Nd^{3+}	$^4F_{3/2} \rightarrow {}^4I_{11/2}$	1.0482	≈ 803	1.1446	[4]
$GdVO_4$	C_{4h}^{19}	Nd^{3+}	$^4F_{3/2} \rightarrow {}^4I_{11/2}$	1.0633	≈ 882 [b]	1.1733	[18]
			$^4F_{3/2} \rightarrow {}^4I_{13/2}$	≈ 1.341	≈ 890	≈ 1.521	[19]
$LuVO_4$	C_{4h}^{19}	Nd^{3+}	$^4F_{3/2} \rightarrow {}^4I_{11/2}$	1.0658	≈ 900 [c]	1.1788	[20]
$BaWO_4$	C_{4h}^6	Nd^{3+}	$^4F_{3/2} \rightarrow {}^4I_{11/2}$	≈ 1.055	≈ 926	≈ 1.169	[21]
$PbMoO_4$	C_{4h}^6	Nd^{3+}	$^4F_{3/2} \rightarrow {}^4I_{11/2}$	1.0594	≈ 869	1.1668	[22]
$PbWO_4$	C_{4h}^6	Nd^{3+}	$^4F_{3/2} \rightarrow {}^4I_{11/2}$	1.0580	≈ 901 [d]	1.1695	[22,23]

[a] Were used articles only in refereed journals.
[b] SRS-promoting mode was established in [24].
[c] SRS-promoting mode was established in [25].
[d] SRS-promoting mode was established in [26].

Table 1 Selected crystalline self-Raman lasers and their SE wavelengths (λ_{SE}), the first Stokes generation wavelengths (λ_{St1}), and SRS promotion vibration modes (ω_{SRS})

design. Nowadays crystalline SRL with laser-diode (LD) pumping are an extensively growing research area in solid-state laser physics, in which are working of many groups of researchers. The selected results of some of these investigations are shown in Table 1.

Mentioned above data indicate convincingly that the search of new Ln^{3+}-ion doped SRS-active crystals is currently a topical task.

In present letter, we report results on the observation high-order SRS in undoped Y_2SiO_5 crystals and on the first performance of a LD-pumped one-micron nanosecond SRL based on the $\chi^{(3)}$-active monoclinic Y_2SiO_5:Nd^{3+} crystal with passively Q-switched generation at single-step cascade SE ($^4F_{3/2} \rightarrow {}^4I_{11/2}$) $\rightarrow$ SRS ($\omega_{SRS1} \approx 904$ cm^{-1}) driving scheme. What is more, for this crystal we achieved with LD-pumping the quasi-CW lasing regime at 1.3585 μm wavelength of its $^4F_{3/2} \rightarrow {}^4I_{13/2}$ intermanifold transition. The achievement dates back to old work of one of us [27], in which for the first time was recorded several SE wavelengths for both laser intermanifold transitions $^4F_{3/2} \rightarrow {}^4I_{11/2}$ and $^4F_{3/2} \rightarrow {}^4I_{13/2}$ at 300 K and 77 K under microsecond Xe-flashlamp pumping. In the same place was noted that other isostructural orthosilicates, in particular Er_2SiO_5 doped with Ho^{3+} and Tm^{3+} ions are also potential SE media. It should be noted here that during the ensuing years included current time in a several research teams were de-

Crystal	Ln^{3+} lasants				
	Nd^{3+}	Ho^{3+}	Er^{3+}	Tm^{3+}	Yb^{3+}
Sc_2SiO_5	[28,29]		[30]		[31]
Y_2SiO_5	[27,28,32,33]	[34]	[35]	[36]	[37]
Gd_2SiO_5 $^{a)}$					[38]
Er_2SiO_5		[34]			
Lu_2SiO_5	[28]	[39]		[40]	[41]
$(Y_{0.5}Gd_{0.5})_2SiO_5$					[42]
$(Y_{0.5}Lu_{0.5})_2SiO_5$					[43]

$^{a)}$ According to [44] the space group for Gd_2SiO_5 doped small concentration of cerium ions ($\approx$0.01 %) is determined as $C_{2h}^5 - P2_1c$ (No. 15).

Table 2 Selected rare-earth C_{2h}^6-monoclinic orthosilicate host-crystals for Ln^{3+} lasants

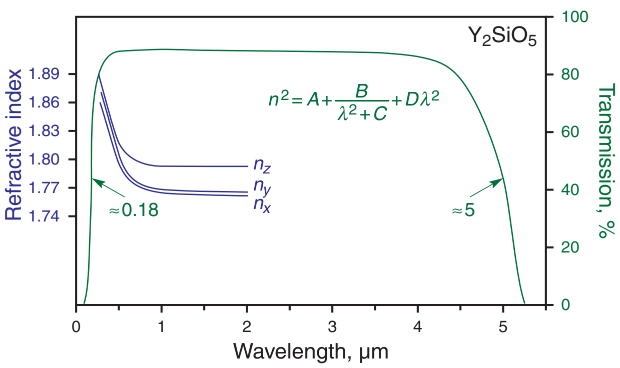

Figure 1 (online color at www.lphys.org) Room-temperature wavelength dispersion of principal refractive indices plotted by the modified Sellmeier equation [48] and transmission spectrum of a monoclinic undoped Y_2SiO_5 single crystal. The arrows indicate the estimated UV and IR transmission limits

(a)

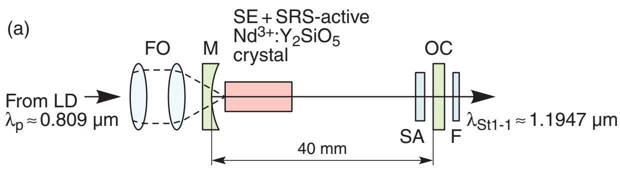

(b)

Reflection (R), transmission (T)

Wavelength, µm	R_M, %	T_M, %	R_{OC}, %	T_{OC}, %
$\lambda_{SE} \approx 1.0782$	≈ 99.5	a)	≈ 99.5	a)
$\lambda_{St1\text{-}1} \approx 1.1947$	≈ 99.4	a)	≈ 60	≈ 40
$\lambda_p \approx 0.809$	≈ 15	85	≈ 10	b)

a) Minor transmission.
b) Lasing crystal absorb almost 100% of pump radiation.

(c)

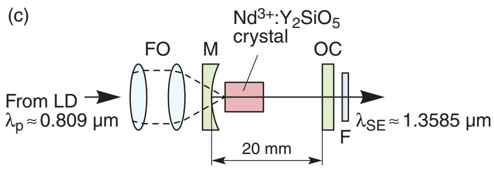

(d)

Reflection (R), transmission (T)

Wavelength, µm	R_M, %	T_M, %	R_{OC}, %	T_{OC}, %
$\lambda_{SE} \approx 1.3585$ ($^4F_{3/2} \to {}^4I_{13/2}$)	≈ 99.5	a)	98	2
$\lambda_{SE} \approx 1.0782$ ($^4F_{3/2} \to {}^4I_{11/2}$)	≈ 15	≈ 85	≈ 15	≈ 85
$\lambda_p \approx 0.809$	≈ 10	≈ 90	≈ 10	b)

a) Minor transmission.
b) Lasing crystal absorb almost 100% of pump radiation.

Figure 2 (online color at www.lphys.org) (a) and (c) – schematic diagrams of LD-pumped Q-switched Nd^{3+}:Y_2SiO_5 self-Raman laser generating through the nonlinear cascade scheme SE($^4F_{3/2} \to {}^4I_{11/2}$) → SRS ($\omega_{SRS1} \approx 904$ cm^{-1}) and quasi-CW Nd^{3+}:Y_2SiO_5 laser emitting at wavelength of the $^4F_{3/2} \to {}^4I_{13/2}$ channel, respectively; (b) and (d) – optical reflection and transmission of cavity components at pumping lasing wavelengths (see also text)

veloped and investigated many new laser rare-earth C_{2h}^6-monoclinic silicates some of them are listed in Table 2. Under different pumping techniques they can generate in CW and pulsed regimes (including femtosecond [45]).

Thanks to suitable spectroscopic properties of the Y_2SiO_5:Nd^{3+}crystal was realized also new type of operating scheme of solid-state lasers – ground-state-depleted scheme which enables to obtain SE on inter-Stark transitions of the $^4F_{3/2} \to {}^4I_{9/2}$ generation channel of Nd^{3+} lasants. In particular, using the bleach-wave pumping at 0.745 μm wavelength of alexandrite ($BeAl_2O_4$:Cr^{3+}) laser in [32] was achieved spectroscopic condition for efficient room-temperature generation at 0.912 μm wavelength. At present, most of the listed in Table 2 rare-earth orthosilicates doped with Yb^{3+} ions are under fixed interest of laser researchers.

2. Crystals and experimental setups

Both undoped and Nd^{3+}-ions doped yttrium orthosilicate single crystals were grown along $\approx \langle 010 \rangle$ direction by the usual Czochralski technique (with pulled rate $\approx$4 mm/h and rotation $\approx$30 min^{-1}) in air using an Ir crucible. From growing boules were fabricated polished oriented along x-axis samples of different sizes for optical, spectroscopic, SRS, and nonlinear-laser measurements. For laser experiments were used crystalline Y_2SiO_5:Nd^{3+} ($C_{Nd} \approx 1$ at.%) elements of different length having wide-band antireflection coating on their working plane-parallel end-faces. The crystallographic and some physical properties of Y_2SiO_5 single crystals a listed in Table 3.

Property	
Space group [46]	$C_{2h}^6 - C2/c$ (No. 15)
Class	2/m
Unit cell parameters, Å [47] $^{a)}$	$a = 14.371$; $b = 6.710$; $c = 10.388$; $\beta = 122.17°$
Number of formula per unit cell	$Z = 8$
Site symmetry (SS) and coordination number (CN) of cations	Y_{I}^{3+}: SS – C_1, CN = 7; Y_{II}^{3+}: SS – C_1, CN = 6; Si^{4+}: SS – C_1, CN = 4
Density, g/cm^3	≈ 4.3
Melting temperature, °C	≈ 2000
Method of crystal growth	Czochralski, flax (see, e.g. [47])
Thermal conductivity, W/cm/K [33]	$k \approx 0.045$
Optical transparency range, μm $^{b)}$	≈ 0.18 – ≈ 0.5 (see Fig. 1)
Refractive index (modified Sellmeier equation) [48] $^{c)}$	$n^2 = A + \frac{B}{\lambda^2 + C} + D\lambda^2$
Linear optical character	biaxial positive ($n_z > n_y > n_x$)
Nonlinearity	$\chi^{(3)}$
Fracture toughness, 10^6 Mpa $m^{1/2}$ [33]	≈ 0.54
Optical damage threshold, J/cm^2 [33] $^{d)}$	≈ 7.6
Extrinsic thermal-stress-resistance figure of merit, W/cm [33]	$R_T \approx 3.8$
Stimulated emission wavelengths of Nd^{3+} ions, μm [27] $^{e)}$	at $^4F_{3/2} \rightarrow {}^4I_{11/2}$ channel: 1.0782, 1.0742, and 1.0715; at $^4F_{3/2} \rightarrow {}^4I_{13/2}$: 1.3585
Lifetime of $^4F_{3/2}$ state of Nd^{3+} ions, μs $^{f)}$	$\tau_{lum}(^4F_{3/2}) \approx 250$
Extension phonon spectra, cm^{-1} $^{g)}$	≈ 970
Energy of SRS-promoting vibration modes, cm^{-1} $^{h)}$	$\omega_{SRS1} \approx 804$; $\omega_{SRS2} \approx 533$
FWHM linewidth of the Raman shifted lines related to SRS-promoting vibration modes, cm^{-1}	$\Delta\nu_{R1} \approx 6$; $\Delta\nu_{R2} \approx 7.5$
Steady-state Raman gain coefficient for the first Stokes lasing at 1.1947 μm wavelength, cm/GW	$g_{ssR}^{St1-1} \approx 2.3$

$^{a)}$ According to [49] these parameters are: $a = 14.407$ Å; $b = 6.727$ Å; $c = 10.417$ Å, and $\beta = 122.19°$.

$^{b)}$ For 1-mm thick ≈ x-cut plate.

$^{c)}$ Sellmeier coefficients: λ is in μm [48]

Index	A	B	C	D
n_x	3.0895	0.0334	0.0043	0.0199
n_y	3.1173	0.0283	–0.0133	0.00
n_z	3.1871	0.0302	–0.0138	0.00

$^{d)}$ Under 15-ns (FWHM) laser pulses at 1.064 μm wavelength.

$^{e)}$ Spectral composition of SE depends on a Nd^{3+}-ion concentration and an orientation of lasing crystal (see, e.g. [50]).

$^{f)}$ For low Nd^{3+}-doping concentration [33].

$^{g)}$ From spontaneous Raman scattering and IR-transmission spectra [51].

$^{h)}$ It is possible that Y_2SiO_5 crystal has also other SRS-active modes.

Table 3 Some known room-temperature physical properties of monoclinic Y_2SiO_5 single crystals

The performance of Q-switched generation regime in self-Raman laser on the base of the monoclinic Y_2SiO_5:Nd^{3+} ($C_{Nd} \approx 1$ at.%, $l = 20$ mm along x-axis, ∅ ≈ 4 mm) orthosilicate was carried out using a "black garnet" ($Y_3Al_5O_{12}$:Ca,Cr) as a saturable absorber (SA) and often-used laser design with LD-pumping (see, e.g. [12,20] and some other references of Table 1). As shown in Fig. 2a, it is composed of a 40-mm long laser cavity with ≈ 50-mm curvature concave "pump" mirror (M) and a flat output coupler (OC) having dichroic multilayer dielectric coatings. As seen, the lasing rod (wrapped in an In foil and mounted tightly in water cooled Cu

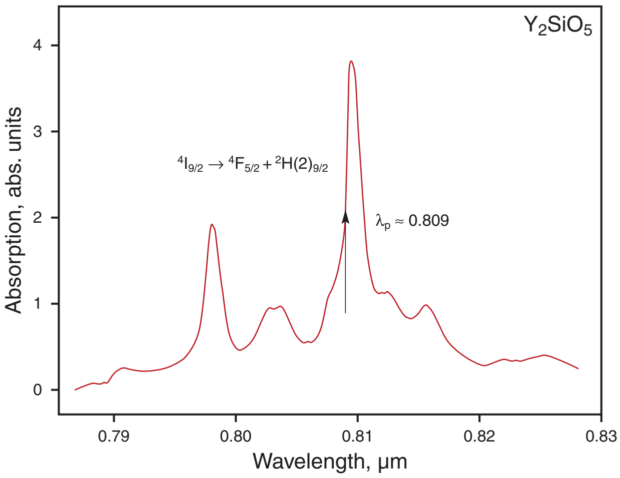

Figure 3 (online color at www.lphys.org) The fragment of room-temperature oriented (along x-axis) absorption spectrum of a monoclinic Nd^{3+}:Y_2SiO_5 single crystal in the pump ($\lambda_p \approx 0.809$ μm) band-area $^4I_{9/2} \rightarrow {}^4F_{5/2} + {}^2H(2)_{9/2}$

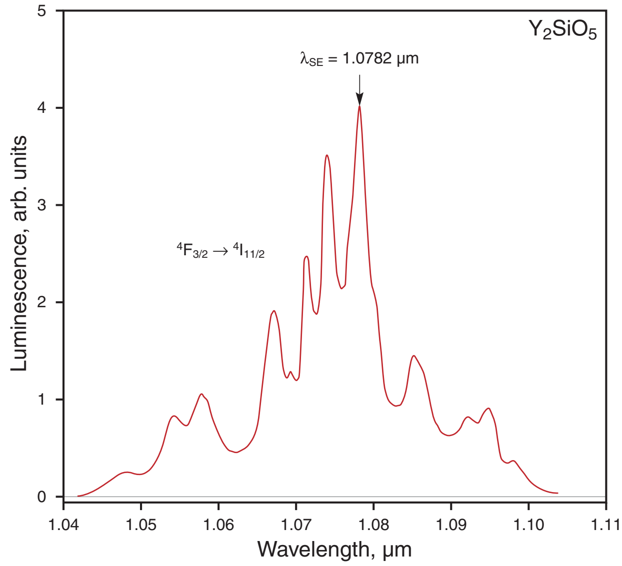

Figure 4 (online color at www.lphys.org) The fragment of room-temperature oriented (along x-axis) luminescence spectrum of a monoclinic Nd^{3+}:Y_2SiO_5 single crystal related to the main SE channel $^4F_{3/2} \rightarrow {}^4I_{11/2}$ of Nd^{3+} lasant ions (see also text)

holder) was positioned near the "pump" mirror. On the other side of the cavity near its OC a commercial 2-mm thick ≈ 1.1 μm wavelength was placed. The pump source was a CW fiber-coupled LD (LIMO GmbH with a core diameter of about 100 μm) having maximum output power of ≈ 5 W at 0.809 μm wavelength. Its relatively wide-band (≈ 15 cm^{-1}) radiation through two-lens focusing optics (FO) with 20-mm focal length and high coupling efficiency was directed into Y_2SiO_5:Nd^{3+} crystal. As shown by Fig. 3, the excitation wavelength is not matched with the maximum of absorption peak of its pumping spectral band-area $^4I_{9/2} \rightarrow {}^4F_{5/2} + {}^2H(2)_{9/2}$. In an effort to achieve quasi-CW operation of titled orthosilicate at SE wavelength of $^4F_{3/2} \rightarrow {}^4I_{13/2}$ intermanifold transition of its Nd^{3+} ions we used, as can be seen from Fig. 2c, very similar laser design with shortened generating Y_2SiO_5:Nd^{3+} ($C_{Nd} \approx 1$ at.%, $l = 10$ mm along x-axis, $\varnothing \approx 4$ mm) crystal and laser cavity (20 mm). The wavelength parameters (reflection and a transmission) of used cavity components are given by small tables in Fig. 2b and Fig. 2d. Spectral composition, average output power, and pulse temporal behavior of developed self-Raman and quasi-CW lasers were measured by universally accepted methods using a grating spectra analyzer (AQ-type), a power meter (Molectron-PM3), and a fast InGaAs PIN photodiode together with a filter (F) and a digital Textronix oscilloscope, respectively.

In the conducted SRS experiments we used undoped Y_2SiO_5 crystalline sample in the form of ≈ 25-mm long (along $\approx x$-axis) rectangular bar (cross-section 4×4 mm^2) with plane-parallel end-faces which have not antireflection coating. Its Raman induced Stokes and anti-Stokes components in the visible and near-IR spectral regions were excited in the single-pass ("cavity free")

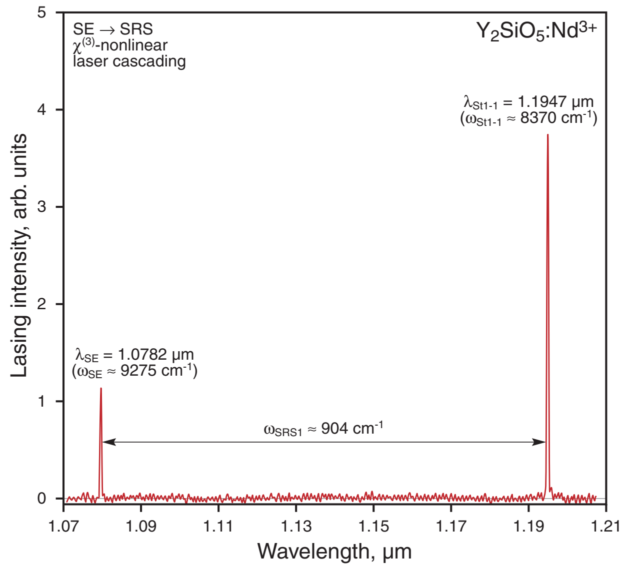

Figure 5 (online color at www.lphys.org) Room-temperature generation spectrum of Q-switched nanosecond Nd^{3+}:Y_2SiO_5 self-Raman laser with its SE ($^4F_{3/2} \rightarrow {}^4I_{11/2}$ channel) and SRS ($\omega_{St1-1} = \omega_{SE} - \omega_{SRS1}$) lines (see also text)

pumping geometry by a homemade Nd^{3+}:$Y_3Al_5O_{12}$ picosecond laser [52] that can emit at two fundamental wavelengths at $\lambda_{f1} = 1.06415$ μm ($\tau_p \approx 110$ ps) and $\lambda_{f2} = 0.53207$ μm (SHG, $\tau_p \approx 80$ ps). Spectral composition of multi-component SRS and Raman-induced four-

Pumping condition		$\chi^{(3)}$-nonlinear lasing lines			SRS-promoting vibration modes, cm^{-1}	
λ_f, μm	Excitation geometry [a)]	Wavelength, μm [b)]	Line [c)]	Line attribution	ω_{SRS1}	ω_{SRS2}
1.06415	$x(zz)x$ (see Fig. 7)	0.7185	ASt_{5-1}	$\omega_{f1}+5\omega_{SRS1}$	≈ 904	
		0.7685	ASt_{4-1}	$\omega_{f1}+4\omega_{SRS1}$	≈ 904	
		0.8258	ASt_{3-1}	$\omega_{f1}+3\omega_{SRS1}$	≈ 904	
		0.8925	ASt_{2-1}	$\omega_{f1}+2\omega_{SRS1}$	≈ 904	
		0.9708	ASt_{1-1}	$\omega_{f1}+\omega_{SRS1}$	≈ 904	
		1.06415	λ_{f1}	ω_{f1}	–	–
		1.1774	St_{1-1}	$\omega_{f1}-\omega_{SRS1}$	≈ 904	
0.53207	$x(\approx y \approx y)x$ (see Fig. 8)	0.4650	ASt_{3-1}	$\omega_{f2}+3\omega_{SRS1}$	≈ 904	
		0.4854	ASt_{2-1}	$\omega_{f2}+2\omega_{SRS1}$	≈ 904	
		0.5077	ASt_{1-1}	$\omega_{f2}+\omega_{SRS1}$	≈ 904	
		0.5174	ASt_{1-2}	$\omega_{f2}+\omega_{SRS2}$		≈ 533
		0.53207	λ_{f2}	ω_{f2}	–	–
		0.5476	St_{1-2}	$\omega_{f2}-\omega_{SRS2}$		≈ 533
		0.5590	St_{1-1}	$\omega_{f2}-\omega_{SRS1}$	≈ 904	
		0.5761	$St_{1-2}St_{1-1}$	$\omega_{f2}-\omega_{SRS1}-\omega_{SRS2}$	≈ 904	≈ 533
		0.5887	St_{2-1}	$\omega_{f2}-2\omega_{SRS1}$	≈ 904	
		0.6218	St_{3-1}	$\omega_{f2}-3\omega_{SRS1}$	≈ 904	
		0.6588	St_{4-1}	$\omega_{f2}-4\omega_{SRS1}$	≈ 904	

[a)] Notation is used in analogy to [53]. The character between parentheses are (from left to right) the polarization of the pumping and of scattering laser radiation, respectively, while the characters to the left and to the right of the parentheses are the pump and the scattering beam direction, respectively. The use of approximate directions is marked "≈".

[b)] Measurement accuracy ± 0.0003 μm.

[c)] Used notation $St_{1-2}St_{1-1}$ is defined as the first Stokes component (related to the second promoting vibration mode $\omega_{SRS2} \approx 533$ cm^{-1}) from the first Stokes lasing with the first promoting vibration mode $\omega_{SRS1} \approx 904$ cm^{-1}.

Table 4 Spectral composition of SRS and Raman induced four-wave mixing (RFWM) nonlinear $\chi^{(3)}$-generation at room temperature in a monoclinic Y_2SiO_5 single crystal with picosecond Nd^{3+}:$Y_3Al_5O_{12}$-laser pumping at fundamental wavelengths $\lambda_{f1} = 1.06415$ μm and $\lambda_{f2} = 0.53207$ μm (SHG)

wave mixing (RFWM) lasing of the Y_2SiO_5 crystal was investigated (details see, e.g. in [26]) with a spectrometric multi-channel analyzer (CSMA) based on a grating monochromator (McPherson in Czerny-Turner arrangement) with linear image Hamamatsu Si-CCD sensor (S3923-1024Q).

3. Self-Raman and quasi-CW lasing in Y_2SiO_5:Nd^{3+} crystals

The main results of the $\chi^{(3)}$-nonlinear single-step cascade SE ($\lambda_{SE} = 1.0782$ μm of ${}^4F_{3/2} \rightarrow {}^4I_{11/2}$ intermanifold transition) → SRS ($\lambda_{St1-1} = 1.1947$ μm of $\omega_{SRS1} \approx 904$ cm^{-1}) in oriented along x-axis Y_2SiO_5:Nd^{3+} crystal ($l = 20$ mm) are illustrated by Fig. 4 – Fig. 6. Under CW excitation at $\lambda_p \approx 0.809$ μm wavelength and with parameters of used laser cavity (see Fig. 2a and Fig. 2b) SE generation of this orthosilicate begins with pumping threshold of about 150 mW at the wavelength of intense luminescence line of the ${}^4F_{3/2} \rightarrow {}^4I_{11/2}$ channel (see Fig. 4). As shown in Fig. 6, at pump power of about 1.5 W arises cascade SE → SRS laser action at $\lambda_{St1-1} = 1.1947$ μm wavelength with Raman shift of $\omega_{SRS1} \approx 904$ cm^{-1} (Fig. 5). At maximum pumping level of about 5 W of used LD the average output power of our self-Raman Y_2SiO_5:Nd^{3+} laser was ≈ 28 mW. It should be noted here that at this pump power the repetition rate and pulse duration at the wavelength of $\chi^{(3)}$-generation were ≈ 16 kHz and ≈ 2 ns, respectively.

The quasi-CW lasing regime of the Y_2SiO_5:Nd^{3+} crystal ($l = 10$ mm, along x-axis) at $\lambda_{SE} = 1.3585$ μm wavelength of the second intermanifold laser channel $F_{3/2} \rightarrow {}^4I_{13/2}$ was realized with chopped pump radiation ($f_p \approx 60$ Hz, $\tau_p \approx 2$ ms $\gg \tau_{lum}$ (${}^4F_{3/2}$) ≈ 250 ms). In this case pumping threshold was measured as ≈ 0.65 W (see Fig. 6). At the increasing of pump level to ≈ 4.2 W was arising also the generation at $\lambda_{SE} = 1.0782$ μm wavelength, which to decreasing of output power at $\lambda_{SE} = 1.0782$ μm. In our experimental condition we can not suppress this generation due to its relatively high SE peak cross-section $\sigma_e^p \approx 10^{-19}$ cm^2 [48].

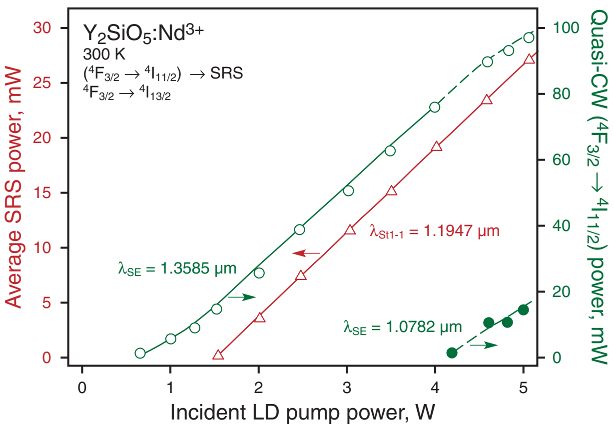

Figure 6 (online color at www.lphys.org) The dependences of the average output power versus incident pump power at $\lambda_p \approx 0.809$ μm wavelength of the nanosecond Nd^{3+}:Y_2SiO_5 self-Raman laser at $\lambda_{St1-1} = 1.1947$ μm (shown by triangles) and of the quasi-CW Nd^{3+}:Y_2SiO_5 laser at wavelengths of $\lambda_{SE} = 1.3585$ μm ($^4F_{3/2} \rightarrow {}^4I_{13/2}$) and $\lambda_{SE} = 1.0782$ μm ($^4F_{3/2} \rightarrow {}^4I_{11/2}$)

4. High-order Stokes and anti-Stokes lasing and SRS-promoting vibration modes

The analysis of the obtained SRS and RFWM spectra under mentioned above picosecond $\chi^{(3)}$-laser experimental arrangements (see Fig. 7 and Fig. 8) of undoped Y_3SiO_5 crystal ($l \approx 25$ mm) is revealed its two SRS-promoting vibration modes. The assignment of all recorded in the visible and near IR-regions Stokes and anti-Stokes lines are summarized also in Table 4.

Since our SRS laser investigation with Y_2SiO_5 crystal was performed under the ss excitation condition $\tau_p \gg T_2 = (\pi \Delta\nu_R)^{-1} \approx 1.7$ ps (here T_2 is the relaxation (dephasing) time of vibration transition and $\Delta\nu_{R1} \approx 6$ cm^{-1} is the linewidth of its Raman shifted line in corresponding spontaneous Raman scattering spectrum (see Fig. 9)) in we can roughly estimate the Raman gain coefficient g_{ssR}^{St1-1} for their first Stokes lasing component $\lambda_{St1-1} = 1.1774$ μm wavelength (related to the first SRS vibration mode $\omega_{SRS1} \approx 904$ cm^{-1}) under one-micron pumping (see Fig. 8 and Table 4). This was done indirectly by the sufficiently tested method (see, e.g. [54]) based on the well known ratio [55] $g_{ssR}^{St1-1} I_p^{thr} l_{SRS} \approx 30$ and a comparison of the "threshold" pump intensity (I_p^{thr}) of the confidently measurable lasing signal at $\lambda_{St1-1} = 1.1774$ μm wavelength for the studied orthosilicate and reference crystal $PbWO_4$ with the same SRS-active length (l_{SRS}) and known gain value $g_{ssR}^{St1} = 3.1 \pm 0.8$ cm/GW [26] for its first Stokes lasing wavelength of $\lambda_{St1} = 1.1770$ μm. Conducted measurement show that the "threshold" pump intensity for the first Stokes component of lead tungstate is about 1.3 time

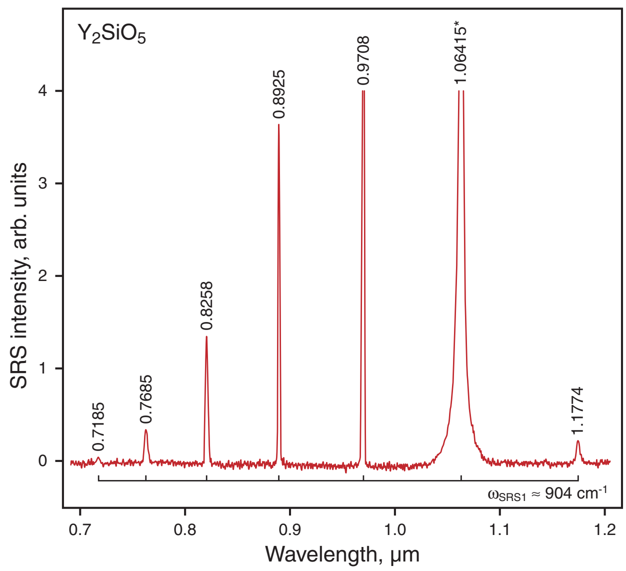

Figure 7 (online color at www.lphys.org) Room-temperature SRS and RFWM spectrum of a monoclinic Y_2SiO_5 crystal recorded in the excitation geometry $x(zz)x$ with picosecond pumping at $\lambda_{f1} = 1.06415$ μm wavelength. The wavelength of all lines (pump line is asterisked) are given in μm, their spectral intensities are shown without correction for the spectral sensitivity of the used analyzing CSMA system with Si-CCD array sensor. The spacing of the Stokes and ant-Stokes lines is a multiple of the single SRS-promoting vibration mode with $\omega_{SRS1} \approx 904$ cm^{-1} of used crystal and is indicated by the horizontal scale brackets

less than for Y_2SiO_5 crystal at $\lambda_{St1-1} = 1.1774$ μm wavelength. Consequently, the value of g_{ssR}^{St1-1} for the orthosilicate is not less than 2.3 cm/GW what indicates that this crystal posses relatively high cubic nonlinear susceptibility. There is reason to believe also that other related monoclinic rare-earth orthosilicates will offer similar $\chi^{(3)}$ nonlinearities. The recent demonstration in [56] a Kerr-lens self-mode-locked Yb^{3+}:$(Y_{0.5}Lu_{0.5})_2SiO_5$ laser confirms this assumption.

The C_{2h}^6 monoclinic unit cell of the Y_2SiO_5 crystal compress 64 atoms (see Table 3) given rise to $3NZ = 192$ degrees of vibration freedom that described by C_{2h}-irreducible representations (in Brillouin-zone center at $\mathbf{k} = 0$) [57] as $\Gamma_{192} = 48A_g + 48B_g + 48A_u + 48B_u$, where the A_g and B_g modes are Raman active, while A_u and B_u modes are IR active. Our analysis of the spontaneous Raman scattering spectra (one of them shown in Fig. 9), as well as the data obtained in Raman studies on Y_2SiO_5 crystal and its isostructural relatives (see, e.g. [51,58]), allow us to conclude that its SRS-promoting mode $\omega_{SRS1} \approx 904$ cm^{-1} belong to the symmetric stretching $A_g(\nu_1)$ vibration of the $(SiO_4)^{4-}$ tetrahedra units and $\omega_{SRS2} \approx 533$ cm^{-1} is the bending ν_4-mode of the $(SiO_4)^{4-}$ units of studies orthosilicate.

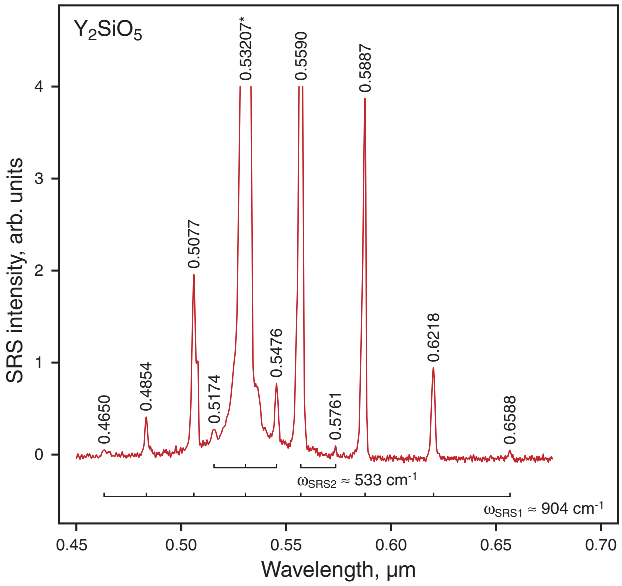

Figure 8 (online color at www.lphys.org) Room-temperature SRS and RFWM spectrum of a monoclinic Y_2SiO_5 crystal recorded in the excitation geometry $x(\approx y \approx y)x$ with picosecond pumping at $\lambda_{f2} = 0.53207$ μm wavelength. The spacing of the Stokes and ant-Stokes lines is a multiple of the SRS-promoting vibration modes with $\omega_{SRS1} \approx 904$ cm^{-1} and $\omega_{SRS2} \approx 533$ cm^{-1} of used crystal and is indicated by the horizontal scale brackets. Used notation as in Fig. 7

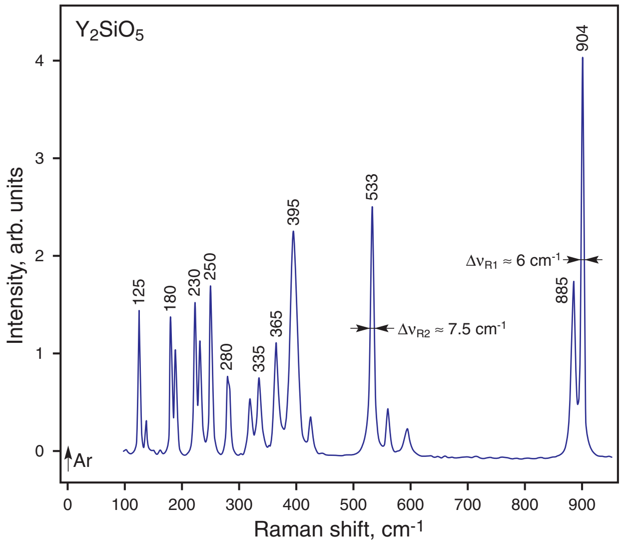

Figure 9 (online color at www.lphys.org) The fragment of polarized spontaneous Raman scattering spectrum of a monoclinic Y_2SiO_5 single crystal recorded at room temperature in the scattering geometry $x(\approx y \approx y)x$ under Ar-ion laser excitation at 0.488 μm wavelength (indicated by an arrow). Intensity of Raman shifted lines are given in cm^{-1} and without correction of sensitivity of the used Hamamatsu R4643 photomultiplier

5. Conclusion

The results of carried out laser and nonlinear-laser studies with Nd^{3+}-ion doped and undoped monoclinic Y_2SiO_5 crystals open up additional properties possibilities for more wide use the rare-earth orthosilicates in modern laser physics and nonlinear optics. It should be noted here that presented numerical values of SE and $\chi^{(3)}$-generation parameters reflect only our current experimental possibilities. They can be significantly enhanced through the optimization of pumping wavelength and all components of laser cavities, as well as by using crystals much better quality and carefully selected their orientation and Nd^{3+}-lasant concentration. Relatively high Raman gain coefficient ($g_{ssR}^{St1-1} \approx 2.3$ cm/GW for Y_2SiO_5) and good thermal conductivity indicate that crystals of this family of monoclinic rare-earth orthosilicates are attractive candidates for Raman laser converters. Thanks to satisfactory ytterbium luminescence properties ($^2F_{5/2} \rightarrow {}^2F_{7/2}$ channel) of these crystals, on the basis of some of them (Y_2SiO_5, Gd_2SiO_5, and Lu_2SiO_5) developed efficient LD-pumped femtosecond lasers [45,59]. In spite of the efforts of many research teams the problem of precise spectroscopic properties of Ln^{3+} ions in C_{2h}^6-monoclinic orthosilicates still remain to be solved. This difficulty related to the structure peculiarity of the crystals. Their trivalent rare-earth host cations and Ln^{3+} lasant ions lie in two different distorted octahedral sites of the C_1 symmetry (see Table 3) as a result of which their absorption and luminescence lines are strongly overlapped. In summary we plane laser experiments to observe other manifestations of nonlinear-laser $\chi^{(3)}$-interactions in Y_2SiO_5 crystals.

Acknowledgements The authors wish to note that this research was considerably enhanced through mutual scientific help within the “Joint Open Laboratory for Laser Crystals and Precise Laser Systems” and supported by the University of Electro-Communications, the Xiamen University, and the Technical University of Berlin. The Russian co-authors are grateful also for partly support by their institutes, as well as by the Russian Foundation for Basic Research and the Program of the Presidium of Russian Academy of Sciences “Extreme light fields and their applications”. Authors acknowledge J. Findeisen and G.M.A. Gad for a participation in SRS measurements.

References

[1] K. Andryunas, Yu. Vishchakas, V. Kabelka, I.V. Mochalov, A.A. Pavlyuk, G.T. Petrovskii, and V. Syrus, JETP Lett. **42**, 410 (1985).
[2] A.A. Demidovich, A.S. Grabtchikov, A.N. Kuzmin, V.A. Lisinetskii, and V.A. Orlovich, Eur. Phys. J. Appl. Phys. **19**, 113 (2002).
[3] L.S. Wu, A.H. Wang, J.M. Wu, L. Wei, G.X. Zhu, and S.T. Ying, Electron. Lett. **31**, 1151 (1995).
[4] A.A. Kaminskii, Laser Photon. Rev. **1**, 93 (2007).
[5] A.A. Kaminskii, N.S. Ustimenko, A.V. Gulin, S.N. Bagaev, and A.A. Pavlyuk, Doklady Phys. **43**, 148 (1998).

[6] A.M. Ivanyuk, P.A. Shachverdov, V.D. Belyev, M.A. Ter-Pogosyan, and V.L. Ermolaev, Opt. Spectrosc. **59**, 573 (1985); T. Omatsu, Y. Ojima, H.M. Pask, J.A. Piper, and P. Dekker, Opt. Commun. **232**, 327 (2004); A. Hamano, S. Pleasants, M. Okida, M. Itoh, T. Yatagai, T. Watanabe, M. Fujii, Y. Iketaki, K. Yamamoto, and T. Omatsu, Opt. Commun. **260**, 675 (2006).
[7] A.V. Gulin, G.I. Narkhova, and N.S. Ustimenko, Quantum Electron. **28**, 804 (1998).
[8] N.S. Ustimenko and A.V. Gulin, Instrum. Exp. Tech. **41**, 386 (1998); J.H. Huang, J.P. Lin, R.B. Su, J.H. Li, H. Zheng, C.H. Xu, F. Shi, Z.Z. Lin, J. Zhuang, W.R. Zeng, and W.X. Lin, Opt. Lett. **32**, 1096 (2007).
[9] N.S. Ustimenko and E.M. Zabotin, Instrum. Exp. Tech. **48**, 239 (2005).
[10] A.A. Lagatsky, A. Abdolvand, and N.V. Kuleshov, Opt. Lett. **25**, 616 (2000).
[11] J.H. Liu, U. Griebner, V. Petrov, H.J. Zhang, J.X. Zhang, and J.Y. Wang, Opt. Lett. **30**, 2427 (2005).
[12] A.A. Kaminskii, J. Dong, K. Ueda, M. Bettinelli, M. Grinberg, and D. Jaque, Laser Phys. Lett. **6**, 782 (2009).
[13] A.A. Kaminskii, S.N. Bagaev, K. Ueda, K. Takaichi, and H.J. Eichler, Crystallogr. Rep. **47**, 653 (2002).
[14] H. Jelínková, J. Šulc, T.T. Basiev, P.G. Zverev, and S.V. Kravtsov, Laser Phys. Lett. **2**, 4 (2005).
[15] Y.F. Chen, Opt. Lett. **29**, 2172 (2004); X.H. Chen, X.Y. Zhang, Q.P. Wang, P. Li, and Z.H. Cong, Laser Phys. Lett. **6**, 26 (2009).
[16] Y.F. Chen, Opt. Lett. **29**, 1915 (2004); Y.T. Chang, K.W. Su, H.L. Chang, and Y.F. Chen, Opt. Express **17**, 4330 (2009).
[17] V.E. Kisel, A.E. Troshin, N.A. Tolstik, V.G. Shcherbitsky, N.V. Kuleshov, V.N. Matrosov, T.A. Matrosova, and M.I. Kupchenko, Appl. Phys. B **80**, 471 (2005).
[18] T.T. Basiev, S.V. Vassiliev, V.A. Konjushkin, V.V. Osiko, A.I. Zagumennyi, Y.D. Zavartsev, S.A. Kutovoi, and I.A. Shcherbakov, Laser Phys. Lett. **1**, 237 (2004).
[19] Y.F. Chen, Opt. Lett. **29**, 2632 (2004).
[20] A.A. Kaminskii, M. Bettinelli, J. Dong, D. Jaque, and K. Ueda, Laser Phys. Lett. **6**, 374 (2009).
[21] M.E. Doroshenko, T.T. Basiev, S.V. Vassiliev, L.I. Ivleva, V.K. Komar, M.B. Kosmyna, H. Jelínková, and J. Šulc, Opt. Mater. **30**, 54 (2007).
[22] A.A. Kaminskii, S.N. Bagayev, K. Ueda, H.J. Eichler, J. Garcia-Sole, D. Jaque, J.J. Romero, J. Fernandez, R. Balda, A.V. Butashin, and F. Agullo-Rueda, Laser Phys. **11**, 1142 (2001).
[23] W.B. Chen, Y. Inagawa, T. Omatsu, M. Tateda, N. Takeuchi, and Y. Usuki, Opt. Commun. **194**, 401 (2001).
[24] A.A. Kaminskii, K. Ueda, H.J. Eichler, Y. Kuwano, H. Kouta, S.N. Bagaev, T.H. Chyba, J.C. Barnes, G.M.A. Gad, T. Murai, and J. Lu, Opt. Commun. **194**, 201 (2001).
[25] A.A. Kaminskii, H. Rhee, H.J. Eichler, K. Ueda, K. Oka, and H. Shibata, Appl. Phys. B **93**, 865 (2008).
[26] A.A. Kaminskii, C.L. McCray, H.R. Lee, S.W. Lee, D.A. Temple, T.H. Chyba, W.D. Marsh, J.C. Barnes, A.N. Annanenkov, V.D. Legun, H.J. Eichler, G.M.A. Gad, and K. Ueda, Opt. Commun. **183**, 277 (2000).
[27] Kh.S. Bagdasarov, A.A. Kaminskii, A.M. Kevorkov, A.M. Prokhorov, S.É. Sarkisov, and T.A. Tevosyan, Sov. Phys. Dokl. **18**, 664 (1974); A.A. Kaminskii, T.I. Butaeva, A.M. Kevorkov, V.A. Fedorov, A.G. Petrosyan, and M.M. Gritsenko, Inorg. Mater. **12**, 1238 (1976).
[28] A.M. Tkachuk, A.K. Przhevusskii, L.G. Morozova, A.V. Politimova, M.V. Petrov, and A.M. Korovkin, Opt. Spectrosc. **60**, 176 (1986).
[29] L.H. Zheng, J. Xu, L.B. Su, H.J. Li, Q.G. Wang, W. Ryba-Romanowski, R. Lisiecki, and F. Wu, Opt. Lett. **34**, 3481 (2009).
[30] L. Fornasiero, K. Petermann, E. Heumann, and G. Huber, Opt. Mater. **10**, 9 (1998).
[31] P.-H. Haumesser, R. Gaumé, B. Viana, and D. Vivien, J. Opt, Soc. Am. B **19**, 2365 (2002); L. Zheng, J. Xu, G. Zhao, L. Su, F. Wu, and X. Liang, Appl. Phys. B **91**, 443 (2008).
[32] R. Beach, G. Albrecht, R. Solarz, W. Krupke, B. Comaskey, S. Mitchell, C. Brandle, and G. Berkstresser, Opt. Lett. **15**, 1020 (1990).
[33] B. Comaskey, G.F. Albrecht, R.J. Beach, B.D. Moran, and R.W. Solarz, Opt. Lett. **18**, 2029 (1993); B. Comaskey, G.F. Albrecht, S.P. Velsko, and B.D. Moran, Appl. Opt. **33**, 6377 (1994).
[34] A.M. Morozov, M.V. Petrov, V.R. Startsev, A.M. Tkachuk, and P.P. Feofilov, Opt. Spectrosc. **41**, 541 (1976).
[35] C. Li, R. Moncorgé, J.C. Souriau, C. Borel, and Ch. Wyon, Opt. Commun. **107**, 61 (1994); T. Schweizer, T. Jensen, E. Heumann, and G. Huber, Opt. Commun. **118**, 557 (1995).
[36] C. Li, J.-C. Souriau, and R. Moncorge, J. Phys. IV France **1**, C7-371 (1991); C. Li, R. Moncorgé, J.C. Souriau, and Ch. Wyon, Opt. Commun. **101**, 356 (1993).
[37] R. Gaume, P.H. Haumesser, B. Viana, D. Vivien, B. Ferrand, and G. Aka, Opt. Mater. **19**, 81 (2002); M. Jacquemet, F. Balembois, S. Chénais, F. Druon, P. Georges, R. Gaumé, and B. Ferrand, Appl. Phys. B **78**, 13 (2004).
[38] W.X. Li, H.F. Pan, L.E. Ding, H.P. Zeng, G.J. Zhao, C.F. Yan, L.B. Su, and J. Xu, Opt. Express **14**, 686 (2006); C.F. Yan, G.J. Zhao, L.H. Zhang, J. Xu, X.Y. Liang, D. Juan, W.X. Li, H.F. Pan, L.G. Ding, and H.P. Zeng, Solid State Commun. **137**, 451 (2006).
[39] X.M. Duan, B.Q. Yao, L. Ke, Y.L. Ju, and Y.Z. Wang, Laser Phys. Lett. **6**, 715 (2009).
[40] B.Q. Yao, L.L. Zheng, X.M. Duan, Y.Z. Wang, G.J. Zhao, and Q. Dong, Laser Phys. Lett. **5**, 714 (2008).
[41] M. Jacquemet, C. Jacquemet, N. Janel, F. Druon, F. Balembois, P. Georges, J. Petit, B. Viana, D. Vivien, and B. Ferrand, Appl. Phys. B **80**, 171 (2005).
[42] J. Du, X.Y. Liang, Y. Xu, R.X. Li, Z.Z. Xu, C.F. Yan, G.J. Zhao, L.B. Su, and J. Xu, Opt. Express **14**, 3333 (2006); W.X. Li, Q. Hao, L.E. Ding, G.J. Zhao, L.H. Zheng, J. Xu, and H.P. Zeng, IEEE J. Quantum Electron. **44**, 567 (2008).
[43] W.X. Li, S.X. Xu, H.F. Pan, L.G. Ding, H.P. Zeng, W. Lu, C.L. Guo, G.J. Zhao, C.F. Yan, L.B. Su, and J. Xu, Opt. Express **14**, 6681 (2006).
[44] M.Y. Jie, G.J. Zhao, X.H. Zeng, L.B. Su, H.Y. Pang, X.M. He, and J. Xu, J. Cryst. Growth **277**, 175 (2005).
[45] F. Thibault, D. Pelenc, F. Druon, Y. Zaouter, M. Jacquemet, and P. Georges, Opt. Lett. **31**, 1555 (2006).
[46] B.A. Maximov, V.V. Ilyukhin, Yu.A. Kharitonov, and N.V. Belov, Sov. Phys. Crystalogr. **15**, 806 (1970).
[47] N.I. Leonyuk, E.L. Belokoneva, G. Bocelli, L. Righi, E.V. Shvanskii, R.V. Henrykhson, N.V. Kulman, and D.E. Kozhbakhteeva, J. Cryst. Growth **205**, 361 (1999).
[48] R. Beach, M.D. Shinn, L. Davis, R.W. Solarz, and W.F. Krupke, IEEE J. Quantum Electron. **26**, 1405 (1990).

[49] R. Gaume, B. Viana, J. Derouet, and D. Vivien, Opt. Mater. **22**, 107 (2003).
[50] A.A. Kaminskii, Laser Crystals, Their Physics and Properties (Springer, Berlin, 1981 and 1990).
[51] S. Campos, A. Denoyer, S. Jandl, B. Viana, D. Vivien, P. Loiseau, and B. Ferrand, J. Phys.: Condens. Matter **16**, 4579 (2004).
[52] H.J. Eichler and B. Liu, Opt. Mater. **1**, 21 (1992).
[53] T.C. Damen, S.P.S. Porto, and B. Tell, Phys. Rev. **142**, 570 (1966); J.F. Scott and S.P.S. Porto, Phys. Rev. **161**, 903 (1967).
[54] A.A. Kaminskii, L. Bohatý, P. Becker, H.J. Eichler, and H. Rhee, Phys.-Uspekhi **51**, 899 (2008); A.A. Kaminskii, M. Bettinelli, A. Speghini, H. Rhee, H.J. Eichler, and G. Mariotto, Laser Phys. Lett. **5**, 367 (2008); A.A. Kaminskii, L. Bohatý, P. Becker, P. Held, H. Rhee, H.J. Eichler, and J. Hanuza, Laser Phys. Lett. **6**, 335 (2009); A.A. Kaminskii, S.N. Bagayev, V.V. Dolbinina, A.E. Voloshin, H. Rhee, H.J. Eichler, and J. Hanuza, Laser Phys. Lett. **6**, 544 (2009); A.A. Kaminskii, L. Bohatý, P. Becker, H.J. Eichler, H. Rhee, and J. Hanuza, Laser Phys. Lett. **6**, 872 (2009).
[55] W. Kaiser and M. Maier, in: F.T. Arichi and E.O. Shultz-Dubois (eds.), Laser Handbook, vol. 2 (North-Holland, Amsterdam, 1972), p. 1007; Y.R. Shen, The Principles of Nonlinear Optics (Wiley, New York, 1984).
[56] J. Liu, W.W. Wang, C.C. Liu, X.W. Fan, L.H. Zheng, L.B. Su, and J. Xu, Laser Phys. Lett. **7**, 104 (2010).
[57] D.L. Rousseau, R.P. Bauman, and S.P.S. Porto, J. Raman Spectrosc. **10**, 253 (1981).
[58] L.H. Zheng, G.J. Zhao, C.F. Yan, X.D. Xu, L.B. Su, Y.J. Dong, and J. Xu, J. Raman Spectrosc. **38**, 1421 (2007); D. Chiriu, N. Faedda, A.G. Lehmann, P.C. Ricci, A. Anedda, S. Desgreniers, and E. Fortin, Phys. Rev. B **76**, 054112 (2007); A. Denoyer, S. Jandl, B. Viana, O. Guillot-Noël, P. Goldner, D. Pelenc, and F. Thibault, Opt. Mater. **30**, 416 (2007).
[59] W.X. Li, Q. Hao, H. Zhai, H.P. Zeng, W. Lu, G.J. Zhao, L.H. Zheng, L.B. Su, and J. Xu, Opt. Express **15**, 2354 (2007).